ChemComm

RSC Publishing

COMMUNICATION

Synthesis of atomic metal clusters on nanoporous alumina†

Cite this: *Chem. Commun.*, 2013, **49**, 11317

Received 19th September 2013, Accepted 11th October 2013

DOI: 10.1039/c3cc47170e

www.rsc.org/chemcomm

Ana Sol Peinetti, Santiago Herrera, Graciela A. González* and Fernando Battaglini*

The synthesis of atomic metal (gold and nickel) clusters by pulsed galvanostatic electrodeposition on nanoporous alumina is presented. The method allows the production of clusters with an average diameter of 0.7 nm for gold and 1.1 nm for nickel, while the size can be controlled through the current density applied. This strategy represents a simple and efficient method for the construction of heterogeneous catalysts and sub-nanometre electrode arrays exemplified here by the reduction of 4-nitrophenol and the electrochemical response to ferrocyanide.

In the last few years different reports on the synthesis of sub-nanometre sized metal particles have been presented. These aggregates of metallic atoms involving from 2 to 100 atoms per particle are denominated atomic clusters or nanoclusters. Different electronic, optical, chemical and catalytic properties with respect to metal nanoparticles have been reported.[1–7]

In a recent review, Lu and Chen have pointed out that size-controlled synthesis is one of the big challenges facing the production of this type of system.[8] Most of the used methods are usually carried out in solution phase by controlling different experimental parameters such as the metal to ligand ratio, chemical structure of the protecting ligands, the type of reducing agent, stirring conditions, reaction temperature, time and pH among others. An alternative is the use of templates allowing the control of size and shape; however most of the methods are carried out in solution using high molecular weight species such as polymers,[9,10] polyelectrolytes,[11] proteins,[12] dendrimers[13,14] and DNA.[15] Also, electrochemical methods can be used to get better control of the size; all of them are based on the use of a sacrificial anode as the metal source, carrying out the electrolysis in an organic solvent under an argon atmosphere.[16,17] On the other hand, the electrosynthesis of different types of nanostructures on a solid support has been developed on alumina templates.[18] Nielsch *et al.*[18d] have introduced a metal deposition method onto ordered alumina pores by pulsed electrodeposition. Briefly, the method consisted of: (I) the creation of an oxide nanoporous structure, (II) the chemical etching of the oxide barrier layer, (III) further thinning of the barrier layer by two current-limited anodization steps and (IV) pulsed electrodeposition of metals in the pores. Steps II and III are very important to decrease the electrical insulation produced by the oxide layer, and particularly step III allows the formation of dendritic pores at the barrier layer; this is a key point in the successful filling of the pores with a metal, since the split-up of the pores in the layer between the ordered alumina structure and the aluminium substrate favours the formation of several nucleation sites in each pore at the beginning of the electrodeposition.

Taking this hypothesis into account, in this communication we present the production of atomic nickel and gold cluster nanostructures based on hexagonally arranged porous alumina as a matrix structure. To achieve this goal we decided to follow a similar procedure to the one presented by Nielsch *et al.* avoiding step III, reducing in this way the cites of nucleation points and decreasing the chances of the nuclei to collapse in a bigger structure.

The cluster synthesis is schematized in Fig. 1. Aluminium 1145 was used for the generation of hexagonally ordered porous alumina yielding a nanoporous structure of 10 nm pore diameter, 1 μm depth and a 35 nm interpore spacing. Then, the system is exposed to the metal plating bath and a pulsed electrodeposition sequence is applied (see ESI† for a detailed description).

In the initial experiments we tested gold electrodeposition, employing a $KAu(CN)_2$ solution. After gold deposition, no changes in colour are observed in the surface, a typical feature when alumina nanopores are filled with a metal, evidencing the importance of step III in the method previously mentioned. The analysis of the nanoporous alumina by SEM did not show any evidence of the presence of gold. The same result was observed for Ni electrodeposited from a solution containing $NiSO_4$ and $NiCl_2$ at pH 4.5. In order to obtain a positive proof of the atomic cluster formation, both systems were exposed to 4-nitrophenol in the presence of $NaBH_4$ to determine its ability to catalyze its reduction.[19] In Fig. 2 the changes in a solution containing these

INQUIMAE, Departamento de Química Inorgánica, Analítica y Química Física, Facultad de Ciencias Exactas y Naturales, Universidad de Buenos Aires, Ciudad Universitaria, Pabellón 2, C1428EHA, Buenos Aires, Argentina. E-mail: graciela@qi.fcen.uba.ar, battagli@qi.fcen.uba.ar

† Electronic supplementary information (ESI) available: Details on synthesis of clusters, AFM for Ni clusters, $NaBH_4$ catalytic reduction of 4-nitrophenol and electrochemical reduction of 4-nitrophenol. See DOI: 10.1039/c3cc47170e

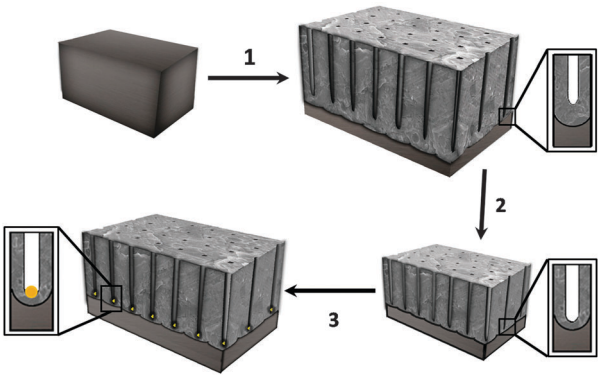

Fig. 1 Cluster synthesis scheme. (1) Aluminium anodization, (2) etching of the oxide barrier, (3) metal pulsed electrodeposition. Fgures not drawn to scale.

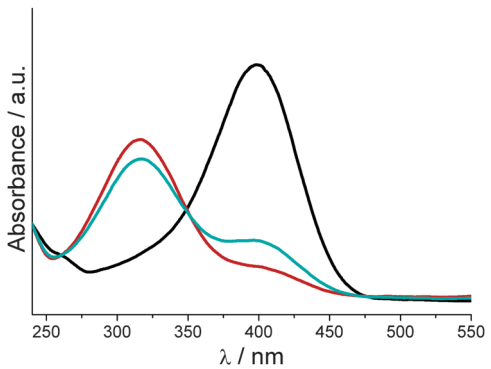

Fig. 2 UV-visible absorption spectra obtained after the reaction of 4-nitrophenol with $NaBH_4$ in the presence of: Al/Al_2O_3 (black line), $Al/Al_2O_3/Au_n$ (red line), and $Al/Al_2O_3/Ni_n$ (cyan line). The absorbance peaks at 405 nm and 314 nm correspond to 4-nitrophenol and 4-aminophenol, respectively.

two reagents exposed to metal modified alumina ($Al/Al_2O_3/Au_n$ and $Al/Al_2O_3/Ni_n$), and, as a blank experiment, alumina (Al/Al_2O_3) can be observed. For both metals a clear change in the absorbance is observed that corresponds to the formation of 4-aminophenol; while for the blank experiment no changes were observed, giving strong evidence of the presence of very tiny particles of metal deposited on nanoporous alumina.

Recently, pseudo-first order rate constants for the same reaction catalysed by $Au_{25}L_{18}$ clusters (where L corresponds to different ligands) were presented.[20] Following the same procedure the pseudo-first order constant for each cluster was determined (see ESI,† Table S1 and Fig. S1). To make the results comparable, we took into account the $NaBH_4$ concentration and the catalyst mass in the reaction volume of the experiment; in this way an apparent rate constant per molar concentration of each of these species can be calculated. Under these conditions, in our case the apparent rate constant is 6×10^8 s^{-1} M^{-2}, which is 50 times higher than the value calculated from the data obtained with Au_{25} clusters.[20]

UV-vis spectroscopy can be a useful tool for probing the gold nanoparticle core size. For particles above 1.5 nm a surface plasmon band appears at around 550 nm. In the case of particles below 1.5 nm, this band disappears and the spectrum shows a continuous increase in absorbance with decreasing wavelength. With a further decrease in size (nanometers to sub-nanometers), the emergence of discrete peaks in the UV region

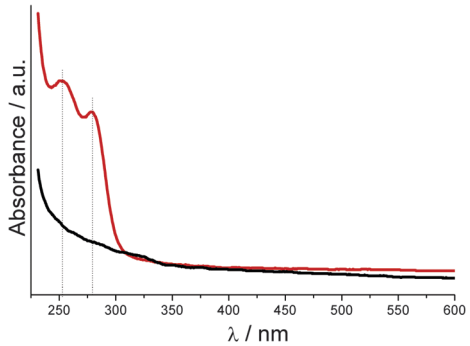

Fig. 3 UV-visible absorption spectra of gold clusters (red line), and, as a blank experiment, a solution containing dissolved Al_2O_3 (black line).

is observed, corresponding to a transition from a bulk-like metallic density of states to an electronic structure described by discrete molecule-like electronic levels.[6,21,22] Fig. 3 shows the spectrum of the dissolved Al_2O_3/Au_n; no signal is observed in the surface plasmon band region (*ca.* 550 nm), and a notable increase in the signal at low wavelength is observed, indicating the presence of nanoclusters. The presence of a fine structure showing peaks at 254 and 280 nm is close to values observed previously by Lopez-Quintela[6] and Chen[23] for atomic clusters.

The cluster size was determined by atomic force microscopy (AFM) using a diluted solution to avoid cluster aggregation. The AFM image of the gold cluster samples is presented in Fig. 4, nanoclusters with heights of about 0.7 ± 0.2 nm (n = 72) are observed. In a similar fashion, Ni atomic clusters were synthesised at different current values, the cluster size increases as the current increases with diameters of 1.1 and 3.7 nm at currents of 3 and 10 mA cm^{-2}, respectively (see Fig. S3 in ESI†).

Nanoelectrode and microelectrode arrays have gained importance in chemical and biochemical sensor technologies;[24] since atomic gold clusters were electrodeposited, a contact with the conductive aluminium substrate should exist, therefore we can expect that the nanoclusters behave as an array of sub-nanometre electrodes inserted into a porous alumina matrix.

Fig. 5 shows the amperometric response to cyclic voltammetry applied to a ferrocyanide solution using $Al/Al_2O_3/Au_n$, and Al/Al_2O_3. In the presence of gold a sigmoidal curve, typical of an ultramicroelectrode, is observed, while for Al/Al_2O_3 a background current is only observed due to the isolation produced by the oxide layer. Recently, Fontaine *et al.*[25] have summarized the critical geometric parameters that need to be controlled to tune the performance of nanoelectrode arrays,

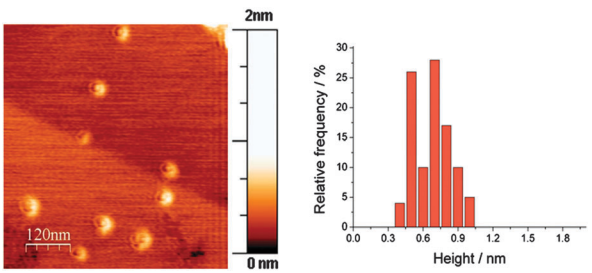

Fig. 4 AFM topography image of gold clusters on the HOPG substrate and the histogram distribution height (section profiles are given in ESI,† Fig. S2).

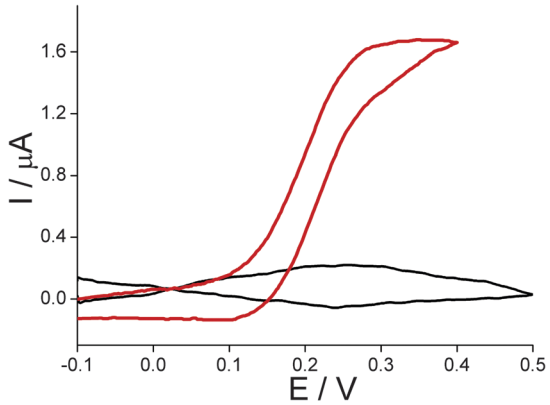

Fig. 5 Cyclic voltammograms at 50 mV s^{-1} in the presence of 50 mM $[Fe(CN)_6]^{4-}$ in buffer HEPES 50 mM at pH 7.0 corresponding to the Al/Al_2O_3 electrode (black line) and the $Al/Al_2O_3/Au_n$ electrode (red line).

they are: the interelectrode spacing, the radius of the nanoelectrode and the recessed or the shape factor (associated with the thickness of the porous layer). Depending on the interplay of these factors and the time scale of the experiment (scan rate), cyclic voltammetry curves will take different shapes. In Fig. S4 (ESI†) the changes in the shape of the voltammogram from a radial diffusion controlled process at slow scan rates to a linear diffusion process at fast scan rates can be observed. This behaviour corresponds to a recessed electrode array; at fast scan rates, the diffusion layer is very small and therefore each electrode behaves as an individual electrode with linear diffusion; meanwhile at slow scan rates, the diffusion layer increases and the shape of the voltammogram takes a sigmoidal shape due to radial diffusion around the pore (see Fig. S5, ESI†). Under the working conditions presented here the pores are not close enough to see again the linear diffusion behaviour due to the collapse of the individual concentration profiles. This means that the length of the diffusion layer is not enough to interconnect all of them, in this way they behave as independent electrodes controlled by radial diffusion. Therefore, at all explored scan rates the observed current is the summation of the individual responses of the atomic gold clusters embedded in a nanoporous alumina structure.

Under radial diffusion conditions (5 mV s^{-1} scan rate), the response of each individual electrode can be calculated using the following expression:[26]

$$i = 2n\pi FCDd^2/(8L + \pi d)$$

where d is the diameter of the electrode, L the length of the pore, C and D the concentration and the diffusion coefficient of the electroactive species, n the number of exchanged electrons and F the Faraday constant. Taking into account the number of pores per square centimetre and the current plateau obtained from the cyclic voltammetry at 5 mV s^{-1}, the average diameter of the gold nanoclusters can be calculated. A value of 0.6 nm is obtained, in agreement with the values previously observed by AFM.

Finally, it is important to point out the good electrocatalytic properties of both metals. Gold and nickel atomic clusters were used for the electrocatalytic reduction of 4-nitrophenol using square wave voltammetry, a technique restricted to species with fast electron transfer kinetics (see Fig. S6 in ESI†), in both cases a clear signal can be observed.

Pulsed galvanostatic electrodeposition on alumina templates allows the synthesis of atomic gold and nickel clusters. The size can be controlled by the current applied as it was demonstrated in the case of nickel. This strategy presents all the advantages of the template-based methods such as simplicity, cluster size control, and high stability against aggregation. Also, due to the lack of stabilizing ligands, the atomic metal clusters can provide non-blocked active surfaces, exemplified here in the efficient reduction of 4-nitrophenol when the array is used either as catalysts or as electrode surfaces. For nanoelectrode array production, this method has the advantage of being both simple and cost effective compared to electron beam lithography,[27] opening new routes for the fabrication of sensors and catalysts using a bottom-up approach.

Notes and references

1 T. G. Schaaff, G. Knight, M. N. Shafigullin, R. F. Borkman and R. L. Whetten, *J. Phys. Chem. B*, 1998, **102**, 10643.
2 M. W. Heaven, A. Dass, P. S. White, K. M. Holt and R. W. Murray, *J. Am. Chem. Soc.*, 2008, **130**, 3754.
3 Y. Negishi, Y. Takasugi, S. Sato, H. Yao, K. Kimura and T. Tsukuda, *J. Am. Chem. Soc.*, 2004, **126**, 6518.
4 E. S. Shibu, M. A. Habeeb Muhammed, T. Tusukuda and T. Pradeep, *J. Phys. Chem. C*, 2008, **112**, 12168.
5 Y.-C. Shiang, C.-C. Huang, W.-Y. Chen, P.-C. Chen and H.-T. Chang, *J. Mater. Chem.*, 2012, **22**, 12972.
6 M. J. Rodriguez-Vazquez, M. C. Blanco, R. Lourido, C. Vazquez-Vazquez, E. Pastor, G. A. Planes, J. Rivas and M. A. Lopez-Quintela, *Langmuir*, 2008, **24**, 12690.
7 S. Hu and X. Wang, *Chem. Soc. Rev.*, 2013, **42**, 5577.
8 Y. Lu and W. Chen, *Chem. Soc. Rev.*, 2012, **41**, 3594.
9 J. G. Zhang, S. Q. Xu and E. Kumacheva, *Adv. Mater.*, 2005, **17**, 2336–2340.
10 Z. Shen, H. W. Duan and H. Frey, *Adv. Mater.*, 2007, **19**, 349–350.
11 L. Shang and S. J. Dong, *Chem. Commun.*, 2008, 1088–1090.
12 J. P. Xie, Y. G. Zheng and J. Y. Ying, *J. Am. Chem. Soc.*, 2009, **131**, 888–889.
13 J. Zheng, J. T. Petty and R. M. Dickson, *J. Am. Chem. Soc.*, 2003, **125**, 7780–7781.
14 J. Zheng and R. M. Dickson, *J. Am. Chem. Soc.*, 2002, **124**, 13982–13983.
15 C. I. Richards, S. Choi, J. C. Hsiang, Y. Antoku, T. Vosch, A. Bongiorno, Y. L. Tzeng and R. M. Dickson, *J. Am. Chem. Soc.*, 2008, **130**, 5038–5039.
16 M. T. Reetz and W. Helbig, *J. Am. Chem. Soc.*, 1994, **116**, 7401.
17 M. J. Rodríguez-Vázquez, M. C. Blanco, R. Lourido, C. Vázquez-Vázquez, E. Pastor, G. A. Planes, J. Rivas and M. A. López-Quintela, *Langmuir*, 2008, **24**, 12690.
18 (*a*) M. S. Sander and H. Gao, *J. Am. Chem. Soc.*, 2005, **127**, 12158; (*b*) M. A. S. Chong, Y. B. Zheng, H. Gao and L. K. Tan, *Appl. Phys. Lett.*, 2006, **89**, 233104; (*c*) J. C. Claussen, M. M. Wickner, T. S. Fisher and D. M. Porterfield, *ACS Appl. Mater. Interfaces*, 2011, **3**, 1765; (*d*) K. Nielsch, F. Müller, A.-P. Li and U. Gösele, *Adv. Mater.*, 2000, **12**, 582.
19 J. Macanás, L. Ouyang, M. L. Bruening, M. Muñoz, J.-C. Remigy and J.-F. Lahitte, *Catal. Today*, 2010, **156**, 181.
20 A. Shivhare, S. J. Ambrose, H. Zhang, R. W. Purvesab and R. W. J. Scott, *Chem. Commun.*, 2013, **49**, 276.
21 G. H. Woehrle, M. G. Warner and J. E. Hutchison, *J. Phys. Chem. B*, 2002, **106**, 9979.
22 Y. Zhu, H. Qian, M. Zhu and R. Jin, *Adv. Mater.*, 2010, **22**, 1915.
23 Y. Yang and S. Chen, *Nano Lett.*, 2003, **3**, 75.
24 D. W. M. Arrigan, *Analyst*, 2004, **129**, 1157.
25 O. Fontaine, C. Laberty-Robert and C. Sanchez, *Langmuir*, 2012, **28**, 3650.
26 B. Zhang, Y. Zhang and H. White, *Anal. Chem.*, 2004, **76**, 6229.
27 N. Godino, X. Borrisé, F. X. Muñoz, F. J. del Campo and R. G. Compton, *J. Phys. Chem. C*, 2009, **113**, 11119.